MOTIVECTION
Journal of Mechanical Electrical and Industrial Engineering

Volume : 6, Number : 3, 2024
ISSN : 2655 – 7215 [printed] ; 2685-2098 [online]
DOI : 10.46574/motivection.v6i3.351

Electrochemical Characterization Techniques for Performance Optimization in Dye-sensitized Solar Cells: A Narrative Review

Teknik Karakterisasi Elektrokimia untuk Optimalisasi Kinerja pada Dye-sensitized Solar Cells: Tinjauan Naratif

Agung Purnomo[1]*, Achmad Aziizudin[1], Arbye S[1], Cahyo Wibi Yogiswara[1], Dimas Ardiansyah Halim[1], Setya Drana Harry Putra[1]

Abstract

Dye-sensitized solar cells (DSSCs) offer advantages such as low production costs, simple fabrication methods, and reduced toxicity compared to silicon-based solar cells, although their efficiency remains a major limitation. The aim of this review is to discuss the fundamental principles of DSSCs and evaluate the electrochemical techniques used to optimize their performance. The method employed is a narrative literature review, allowing the author to synthesize relevant literature from various sources. Current-voltage (I-V) measurements and electrochemical impedance spectroscopy (EIS) are identified as the primary tools for assessing DSSC efficiency and quality. The findings indicate that I-V measurements provide critical metrics such as efficiency and fill factor, while EIS helps identify charge transfer resistance and improves cell stability. Techniques such as voltammetry and Tafel polarization plots offer additional insights into catalytic activity and diffusivity. This review underscores the importance of electrochemical characterization in supporting efficiency improvements and the development of new materials, with EIS playing a key role in modelling cell morphology through equivalent circuit analysis.

Keywords
DSSC, IV measurements, CV measurements, tafel polarization, electrochemical impedance spectroscopy

[1] *Mechanical Engineering Department, Facuty of Engineering, Tidar University*
Jl. Kapten Suparman 39 Potrobangsan,Magelang Utara, Jawa Tengah 56116, Telp. (0293) 364113
* agungpurnomo@untidar.ac.id

Submitted : September 20, 2024. Accepted : November 17, 2024. Published : November 30, 2024.

INTRODUCTION

Many governments and leaders have developed decarbonization frameworks across various regions, stimulating the increased deployment of renewable energy. renewable energy accounted for approximately 18.15% of total final energy consumption. Although it still represents a small portion of overall energy consumption, certain sources, such as photovoltaic (PV) technology, are experiencing rapid growth. According to the trends ad report from the International Energy Agency Photovoltaic Power Systems Programme, PV contributed to 2.9% of global electricity demand in 2018 [1]. One notable example of PV technology is dye-sensitized solar cells (DSSCs).

DSSCs operate by injecting electrons from dye molecules into the conduction band of semiconductor substrates. DSSCs have lower production cost than conventional solar cells. They have lower production costs compared to conventional solar cells and offer advantages such as simple preparation methods, reduced toxicity, and ease of manufacturing. Despite these

strengths, DSSCs face drawbacks, including lower efficiency (around 14%) compared to silicon-based solar cells (efficiencies between 20-30%). This lower efficiency is attributed to several factors, including charge recombination, energy loss at interfaces, electrolyte stability, limitations in light absorption, and material constraints [2]. Extensive research is ongoing to enhance the efficiency of DSSCs [3].

Electrochemical characterization techniques are essential for understanding and optimizing the performance of DSSCs. Efficiency is a critical aspect of performance evaluation for DSSCs, and various characterization methods are employed to assess their capabilities. Methods such as UV-Vis Spectroscopy, X-ray Diffraction (XRD), and Scanning Electron Microscopy (SEM) help determine the properties of the different layers within the cells. The four-point probe system and current-voltage (IV) characteristics are utilized to assess the electrical properties of DSSCs [4]. XRD is instrumental in determining crystal size, while SEM provides insights into surface morphology, which affects dye absorption. UV-Vis spectroscopy helps analyze light absorption across layers [5]. Intensity Modulated Photocurrent Spectroscopy (IMPS) is specifically employed to evaluate the activation of the dye [6]. Another vital method is Electrochemical Impedance Spectroscopy (EIS), which sheds light on degradation mechanisms and the effects of accelerated aging [7]. The enhancement of efficiency heavily relies on understanding recombination resistance and chemical capacitance, both of which can be analyzed using EIS [8].

This review aims to provide a comprehensive analysis of how electrochemical characterization techniques contribute to optimizing the efficiency of DSSCs. By emphasizing the significance of higher-efficiency, the review outlines the evolution of DSSC technology from its inception to the latest advancements. It focuses on the role of electrochemical techniques in enhancing performance and achieving maximum efficiency levels in contemporary DSSCs.

METHOD

This research utilized a narrative review method to provide comprehensive insights into the development of electrochemical analysis in DSSCs. The narrative review approach is well-suited for qualitatively synthesizing diverse literature, allowing for a thorough exploration of various electrochemical techniques and their applications within DSSCs. This method was chosen for its flexibility, as it enables the examination of the context and relevance of these techniques without the constraints imposed by quantitative methodologies.

Relevant literature was selected from a range of reputable databases, including Scopus, Web of Science, and Google Scholar. he selection criteria were based on the pertinence of the articles to the topic and the reputation of the journals. Keywords used in the search included "electrochemical characterization," "DSSC performance optimization," "EIS," "cyclic voltammetry," as well as broader terms such as "photovoltaic," "solar cells," and "dye-sensitized solar cells." The analysis involved a thorough and analytical reading of the journal content to ensure comprehensive coverage of the subject matter.

Inclusion criteria for this review focused on studies that specifically examine the use of electrochemical techniques for the characterization and optimization of DSSCs. Exclusion criteria eliminated studies that were not relevant to DSSCs or that employed non-electrochemical techniques. The review was limited to articles that are contextually related to the electrochemical characterization of DSSCs, particularly emphasizing Electrochemical Impedance Spectroscopy (EIS). The literature discussion is organized into six sections: the first explores the structure and mechanism of DSSCs; the second focuses on cyclic voltammetry; the third addresses photocurrent-voltage measurements; the fourth and fifth sections discuss Tafel polarization and EIS. The final section covers the application of electrochemical

characterization in the development of DSSCs. The last step in the process is the report writing, following the overall methodology outlined by Cronin, as illustrated in Figure 1.

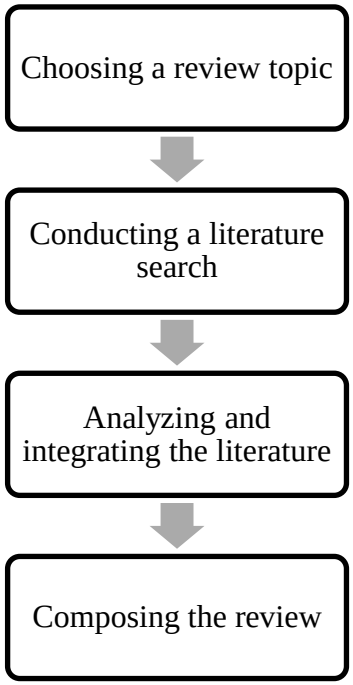

Figure 1. Literature review steps based on Cronin's methodology

RESULTS AND DISCUSSION

The performance of DSSCs can be evaluated using several fundamental electrochemical techniques, including cyclic voltammetry, current-voltage (I-V) measurements, Tafel polarization, and electrochemical impedance spectroscopy (EIS). Before delving into these characterization methods, it is essential to understand the structure and working mechanism of DSSCs to better grasp the objectives of these analyses.

Structure and Mechanism

DSSCs operate function through a photoelectrode mechanism that was initially conceptualized in 1887 and further developed in the 1960s. This mechanism entails the injection of electrons from a dye into an n-type semiconductor substrate. The structure of a DSSC includes several key components: an anode, photoelectrode, p-type quantum dots, dye, electrolyte, catalyst, and cathode, as illustrated in Figure 2a. The anode and cathode typically serve as mechanical supports and are generally made from conductive oxides. The semiconductor film, often composed of titanium dioxide (TiO_2), is combined with a dye sensitizer that is adsorbed onto its surface. The electrolyte solution contains a redox mediator, while the counter electrode (cathode) is responsible for regenerating the redox mediator, commonly using materials such as platinum. The mechanism of DSSCs starts when photons are absorbed by the dye sensitizer, exciting the dye and causing it to inject electrons into the conduction band of the semiconductor. These electrons then move through the semiconductor to the electrode, flow through the external circuit, and return to the back contact [9]. The electrolyte, acting as a redox mediator, facilitates the transport of electrons from the back electrode to the dye and back again. This crucial role ensures the continuous flow of electrons within the cell. The full mechanism of a DSSC, encompassing the role of the electrolyte, is illustrated in Figure 2b.

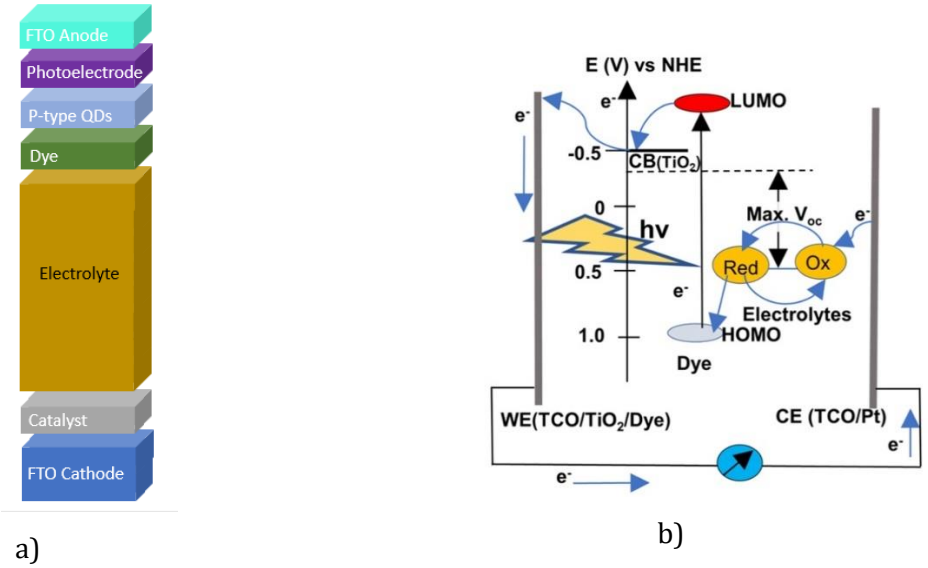

a) b)

Figure 2. Dye sensitized solar cells. (a) structures (b) mechanism [10]

Figure 2b shows the operation of a DSSC, where conducting glass with a TiO_2 layer adsorbs dye molecules. When the dye absorbs photons, it injects electrons into the TiO_2 conduction band. These electrons flow through an external circuit, generating power. An electrolyte with a redox mediator restores the oxidized dye to its original state, with the electrons returning to the counter electrode, typically coated with a catalyst like platinum. The energy alignment between the dye, TiO_2, and electrolyte is shown on a E vs. NHE scale.

Cyclic Voltammetry (CV)

The inclusion of specific chemical elements within the electrolyte and electrodes is essential in determining the characteristics of DSSCs. Cyclic Voltammetry (CV) is used to investigate the electrochemical processes of the dyes, particularly their redox (reduction-oxidation) behavior. To conduct CV, it is essential to prepare an electrochemical cell, choose an appropriate electrolyte, solvent, and sample, set a potential range, and have a solid understanding of data analysis techniques [11]. The CV process can help identify the optimal band gap energies by providing valuable information about electron excitation, which in turn can lead to improved efficiency [12]. CV analysis can be utilized to determine the energy levels of the HOMO (Highest Occupied Molecular Orbital) and LUMO (Lowest Unoccupied Molecular Orbital). The positioning of the HOMO facilitates efficient dye regeneration, contributing to improved solar cell performance [13]. The data from CV analysis can be plotted as a graph of potential versus current, as shown in Figure 3.

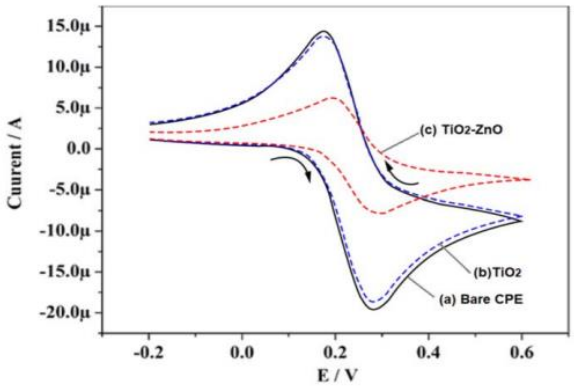

Figure 3. Graph of Cyclic Voltametry [14]

Figure 3 illustrates the oxidation and reduction processes occurring within DSSCs. Positive current is observed at the oxidation peaks, where electrons are transferred from the electrode to the solution, while negative current represents the reduction process, where electrons return to the electrode.

Current-Voltage (I-V) Measurements

I-V measurements, which assess the electrical properties of the solar cell, are conducted under specific conditions since the I-V curve results are influenced by variations in temperature, radiation conditions, and light spectrum. For accurate performance evaluation, these conditions are typically controlled at a standard spectrum such as AM1.5, with a specific irradiance, for example, 100 mW/cm^2, and a fixed temperature, such as 25°C [15]. The representation of these standard measurements, considering temperature, radiation conditions, and spectrum, is illustrated in Figure 3a. Furthermore, the simplified equivalent circuit used for analysis is presented in Figure 3b. The I-V characteristic is a straightforward yet versatile measurement that can determine several key parameters, including the short-circuit current (I_{SC}), open-circuit voltage (V_{OC}), voltage and current at the maximum power point (V_{MP} and I_{MP}), and the maximum output power (P_{MP}). These parameters are essential for deriving important working principles such as the current density (I_0), ideality factor (n), series resistance (R_S), and shunt resistance (R_{SH}). The maximum voltage, maximum current, open-circuit voltage, and short-circuit current can be directly derived from the I-V curve, as shown in Figure 3c. The maximum achievable area can be calculated from the intersection point of the horizontal line representing the open-circuit voltage and the vertical line representing the short-circuit current, as illustrated in Figure 3d.

Figure 3c shows the relationship between current density (mA/cm^2) and voltage (V). Two different materials are being compared: Platinum (black line) and rGO/NiMo Oxide NCs (red line). Platinum demonstrates slightly higher performance, especially at lower voltages, but both materials show a rapid decline in current density after a certain voltage threshold, indicating a similar trend. Figure 3d shows the calculation of Fill Factor (FF) from the I-V curve of a solar cell, where the rectangle at P_MP represents actual power, and the larger rectangle defined by V_{OC} and I_{SC} represents theoretical maximum power. The FF is the ratio of these areas, indicating cell efficiency.

The maximum power can be calculated using these parameters, with the corresponding equation shown in Equation 1. However, specific circuit parameters, including current density, ideality factor, series resistance, and shunt resistance, are not directly measurable as they are inherent and latent [19]. Fortunately, these latent parameters can be determined through mathematical calculations, as outlined in Equations 2 through 4.

$$P_{MP} = V_{MP} \times I_{MP} \tag{1}$$

$$\left[I_{PV} - I - \frac{V}{R_{SH}}\right] = I_0 \exp\left(\frac{qV}{nkT}\right) \tag{2}$$

Symbol q and k are constant. For determining the series resistant and shunt resistant, slope determination can be applied, for R_{SH} slope is around $I=I_{sc}$ and R_S slope is around $V=V_{OC}$ which are given by equation 3 and 4.

$$R_{SH} = -\left(\frac{dV}{dI}\right)_{I=I_{SC}} \tag{3}$$

$$R_S = -\left(\frac{dV}{dI}\right)_{V=V_{OC}} \tag{4}$$

The most important parameter for defining the performance of a DSSCs is efficiency (η). Efficiency refers to the percentage of power from absorbed light that is transformed into electrical energy when the solar cell is connected to an electrical circuit [20]. There are two key concepts when distinguishing efficiency in DSSCs: the semiempirical limit and the detailed balance limit. The semiempirical limit of efficiency is based on the energy gap and empirical constants defined by the Shockley-Queisser model, while the detailed balance limit is grounded in theoretical maximum efficiency. In thermodynamic systems, maximum efficiency is achieved when zero entropy is generated. The ultimate efficiency hypothesis suggests that each photon produces one electronic charge, implying that maximum solar efficiency depends on factors like electron-hole pair generation, radiative recombination, non-radiative losses, electron-hole pair recombination, and charge extraction. In practical applications, the detailed balance limit is commonly applied to estimate the maximum output, typically based on voltage values obtained from the I-V curve [21][22]. The equation used to calculate efficiency the efficiency (η) of DSSCs is presented in Equation 5.

$$\eta = \frac{V_{MP} \times I_{MP}}{P_{INC}} \quad (5)$$

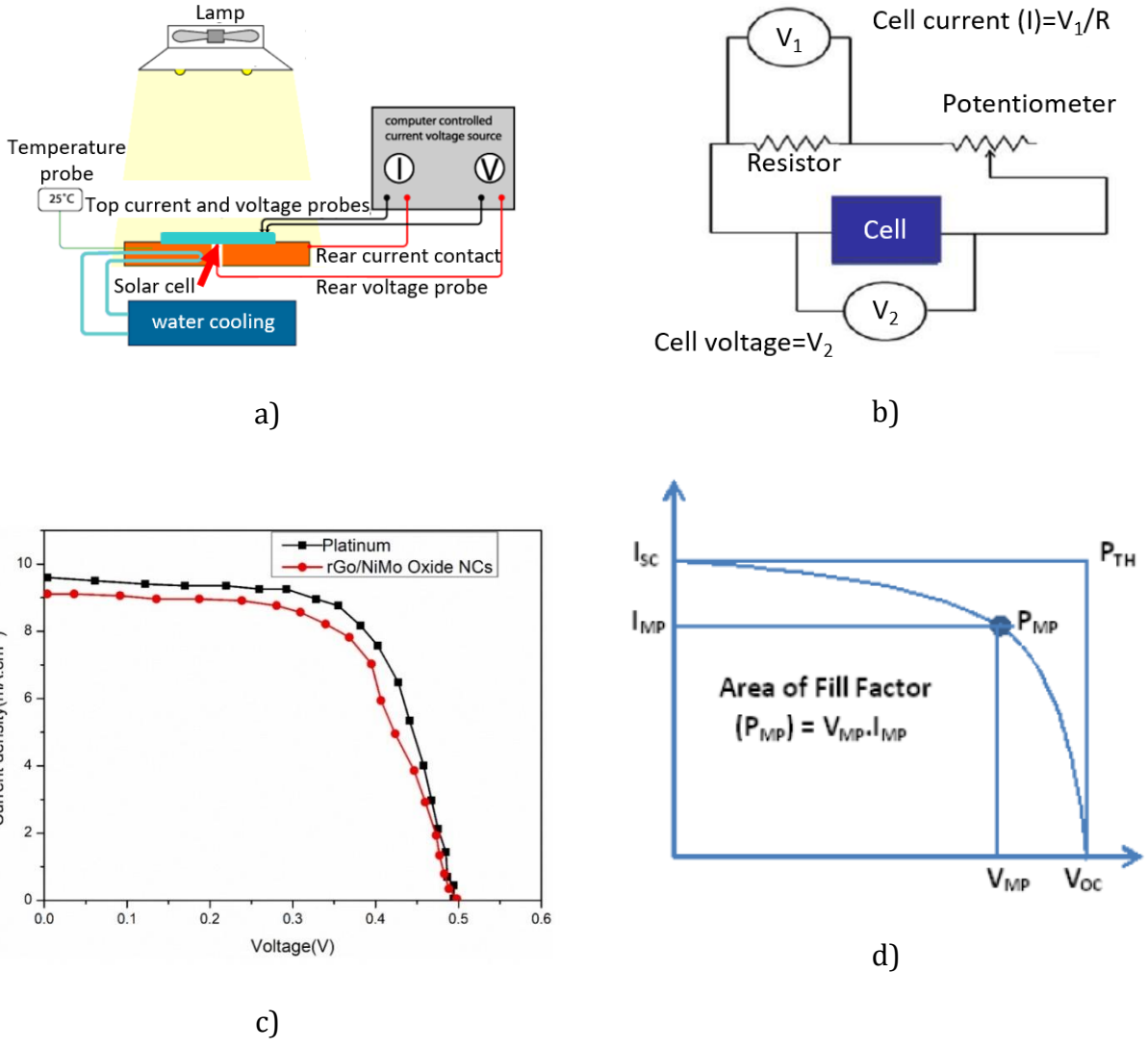

Figure 3. Basic Electrochemical Measurements and Explanations, (a) current voltage measurement, (b) circuit diagram of IV measurement [16], (c) current voltage curve [17], (d) area of fill factor [18].

As previously discussed, determining the highest solar cell efficiency from the current density versus voltage curve requires extracting the exact maximum power point by fitting the curve, as illustrated in Figure 3c. However, fill factor analysis offers an advantage, as it does not require curve fitting [23]. The fill factor (FF) is generally defined as the ratio of the largest rectangle that can fit beneath the I-V curve to the area determined by the short-circuit current density and open-circuit voltage. Highest efficiency of solar cell is obtained from optimization of parameter I_{MP} and V_{MP} so The fill factor equation is represented as Equation 6.

$$FF = \frac{V_{MP} \times I_{MP}}{V_{OC} \times I_{SC}} \quad (6)$$

Tafel Polarization

The performance of DSSCs is closely associated with the quality of the electrodes and their interactions. Exceptional catalytic activity and intrinsic stability are crucial factors for enhancing DSSC efficiency [24]. In DSSCs, the electrocatalytic activity mainly takes place at the interface between the electrode and the electrolyte. Tafel polarization is used to assess the kinetics of electrochemical reactions at the electrode surface, offering insights into both the electrocatalytic activity and the characteristics of interfacial charge transfer [25]. By analyzing the Tafel plots, one can determine the exchange current density and assess the overpotential needed to drive the reaction. Figure 4 illustrates the Tafel polarization plot, highlighting the relationship between overpotential and current density.

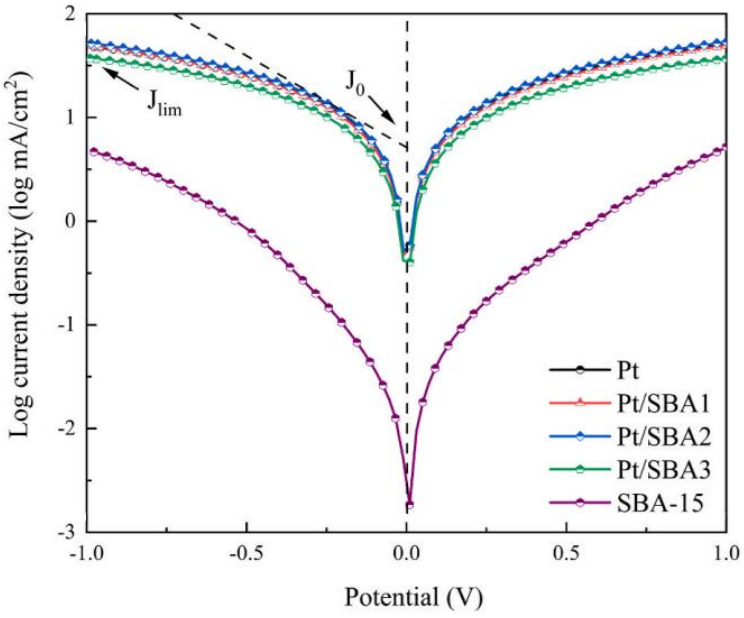

Figure 4. Tafel polarization diagram [26]

The figure 4 represents the logarithmic current density (log mA/cm^2) versus potential (V). Key parameters like J_{lim} (limiting current density) and J_0 (exchange current density) are marked on the graph. The plot compares the performance of various electrodes, for this research, with Pt and its SBA composites showing distinct behaviors in terms of current density and catalytic activity. The steepness and position of the curves provide insight into the electrocatalytic properties and charge transfer efficiencies of these materials.

Electrochemical Impedance Spectroscopy (EIS)

Optimizing DSSCs can be achieved by fine-tuning its physical parameters. Advanced mathematical models, such as electrochemical impedance spectroscopy (EIS), offer a direct approach for analyzing current density-voltage characteristics. In dye-sensitized solar cells,

physical factors like charge transfer, transport, and porosity are intricately linked to the current density and voltage curve, which in turn reflects the cell's overall performance [27]. EIS can also verify electrical resistivity, providing insights into the material's resistance to charge flow within the system [28]. EIS analysis also reveals the role of electron resistance across the shunt, interfaces, and electrolyte solution by evaluating the electron transfer kinetic parameters of each component [29]. Consequently, the equivalent circuit model of a DSSC, based on the cell's morphology, becomes crucial for understanding its performance. By modulating light intensity, EIS helps evaluate electron transport and recombination time constants, essential for optimizing DSSC efficiency by adjusting these rates [30], [31]. The illustration of this model can be seen in Figure 5a. Due to the complexity of the circuit, a simpler equivalent model can be derived by considering only the presence of resistance and capacitance, as shown in Figure 4b.

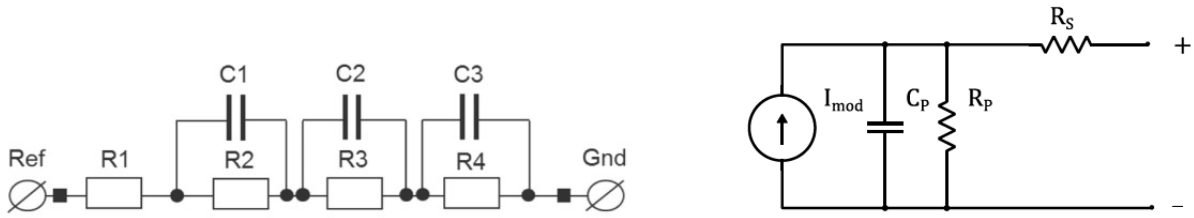

a) b)

Figure 5. (a) equivalent circuit model of DSSC [32], (b) simpler equivalent circuit model [33]

According to the equivalent circuit model graphs in Figures 5a and 5b, impedance measurement is essential for analyzing DSSCs. The results from these measurements are commonly represented as a Nyquist plot, as illustrated in Figures 6a and 6b.

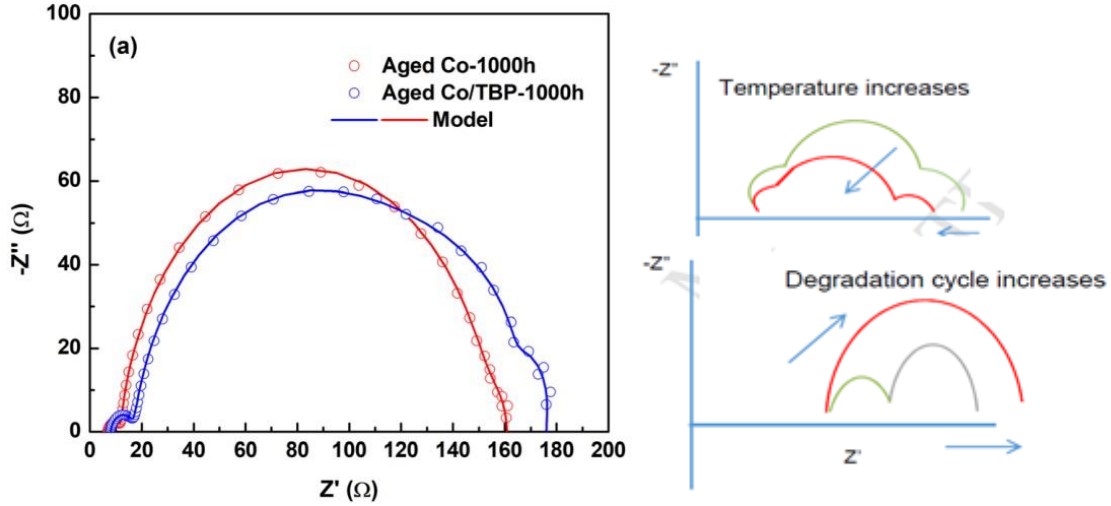

a) b)

Figure 6. Nyquist Plot, (a) Nyquist plot of DSSC [34], (b) effect of temperature and cycle on impedance value [35].

Figure 6a presents Nyquist plots for Aged Co-1000h and Aged Co/TBP-1000h samples, with both datasets fitted to a model for electrochemical impedance behavior. The semicircular nature of the curves indicates the charge transfer resistance (R_{ct}) for each system. The Aged Co-1000h sample exhibits a smaller semicircle compared to Aged Co/TBP-1000h, suggesting a lower charge transfer resistance in the former. This difference implies that the Co-1000h sample has better charge transfer kinetics, potentially resulting in improved electrochemical performance. The model closely fits the experimental data, validating the observed trends. In

DSSC, electrical characterization of electrical properties of materials and interfaces are introduced by charge transfer resistance R_{CT}, capacitance C_{DL} and series resistance R_S [36]. The importance of the Nyquist plot lies in its capacity to demonstrate how various conditions influence changes in dye-sensitized solar cell parameters. As indicated in previous research, Figure 6b shows the impact of increasing temperature (top) and degradation cycles (bottom) on Nyquist plots in electrochemical impedance spectroscopy. As temperature rises, the semicircles expand, indicating increased resistance. Similarly, with more degradation cycles, the semicircles also grow, showing a rise in charge transfer resistance, signaling performance deterioration [35].

The development of EIS has become increasingly valuable as recent advancements, unlike standard EIS, can now detect phenomena occurring at the electrode-electrolyte interface and assess the durability of DSSCs [37]. Additionally, EIS can confirm the cell's performance at the optimal compression temperature [38]. The increase in hydrothermal treatment is directly related to pore size and particle characteristics [39], which is crucial due to DSSCs' exposure to sunlight [40]. Statistical analysis from multiple EIS measurements can improve the reproducibility of DSSCs, ensuring consistent performance and reliability across experiments [41]. Furthermore, simulations can leverage EIS data to develop high-efficiency DSSCs, reducing experimental losses by allowing the evaluation of various electrodes and dyes without extensive physical trials [42]. Although EIS still requires improvements due to the complexity of its measurement system, more autonomous systems are being developed to address these challenges [43].

Application of Electrochemical Characterization in The Development of DSSCs

Over the years, many efforts to enhance the efficiency of DSSCs have yielded limited success, with early methods like increasing semiconductor surface roughness falling short. Since the discovery of TiO_2-based DSSCs, research has focused on optimizing cell performance and stability by refining the photoanode, sensitizer, electrolyte, and counter electrode. The photoanode's porosity and morphology influence dye absorption by increasing the surface area, while the counter electrode provides catalytic activity and conductivity, often enhanced with platinum or conductive polymers. The sensitizer (dye) is key to power conversion, absorbing sunlight and transferring electrons to the semiconductor's conduction band, with performance tied to the dye's molecular structure. Finally, the electrolyte facilitates electron injection and dye regeneration, with its effectiveness influenced by factors such as solvent type, solubility, diffusion rates, recombination kinetics, and redox composition—all critical to the overall efficiency of DSSCs [44].

In 2015, the highest efficiency achieved by a DSSC was 14.7%, utilizing the sensitizer anchor dye ADEKA-1 and the co-sensitizer carboxy-anchor dye LEG4 [45]. The results are summarized in Table 1.

Table 1. Results and Parameters of Highest Efficiency Achieved by DSSCs [45]

Electrolyte: redox[a]	Counter Electrode	Light Intensity ($mWcm^{-2}$)	J_{SC} ($mAcm^{-2}$)	V_{OC} (V)	FF	η (%)
A:I_3^-/I^-	FTO/Pt	100	19.11	0.783	0.748	11.2
F:$[Co(phen)_3]^{3+/2+}$	FTO/Pt	100	17.77	1.018	0.765	13.8
F:$[Co(phen)_3]^{3+/2+}$	FTO/Au/GNP	100	18.27	1.014	0.771	14.3
F:$[Co(phen)_3]^{3+/2+}$	FTO/Au/GNP	50	9.55	0.994	0.776	14.7

The cell structure achieving this highest efficiency is depicted in Figure 7a, where improvements are credited to modifications in the dye, electrolyte, and counter electrode. The combination of ADEKA-1 and LEG4 boosts the incident photon-to-current conversion efficiency

(IPCE), resulting in an increased open-circuit photovoltage (V_{OC}) and short-circuit photocurrent density (JSC). LEG4, when applied to the TiO_2 electrode, acts as a suppressor of back electron transfer and enhances electron distribution, allowing more electrons to move from the dye to the TiO_2 conduction band. Additionally, the electrolyte's impact is influenced by the energy gap between the quasi-Fermi level of TiO_2 and the redox potential of the electrolyte. The cobalt-based electrolyte F:$[Co(phen)_3]^{3+}/^{2+}$, with a higher redox potential than the iodide-based electrolyte A_3^-/I^- yet still below the dye's HOMO levels, provides a stronger thermodynamic driving force for electron regeneration from the electrolyte to the dye, leading to improved photovoltage [45].

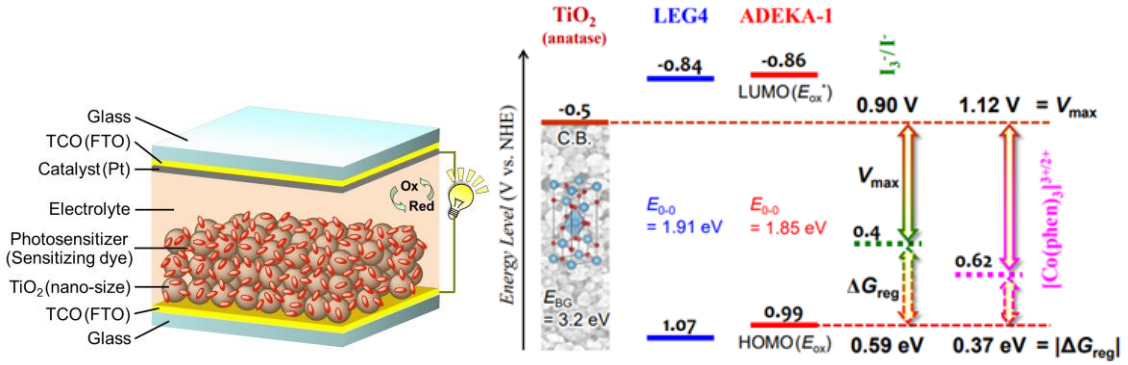

a) b)

Figure 7. (a) DSSC structure with collaborative sensitization by silyl-anchor and carboxy-anchor dyes, and (b) energy level representation [45]

Figures 7a and 7b illustrate that electrochemical measurements can correlate with the physical properties of materials, including molecular structure and energy gap. Differences in molecular structure and energy gap result in variations in open-circuit voltage and short-circuit current. However, this study does not address the relationship between counter electrode type and current density in DSSCs, as prior research has specifically examined counter electrode effects. To evaluate a counter electrode's quality, its electrocatalytic performance can be tested by constructing symmetrical dummy cells, as shown in Figure 8 [46].

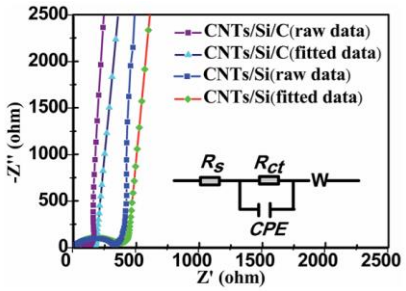

Figure 8. EIS spectrum and the dummy cells [46].

Figure 7 presents a Nyquist plot comparing the electrochemical impedance behavior of CNTs/Si/C and CNTs/Si, with both raw and fitted data. The plot displays the real component (Z') against the imaginary component (-Z''), where the fitted data closely aligns with the raw data for both samples, supporting the equivalent circuit model. This model includes series resistance (R_S), charge transfer resistance (R_{ct}), a constant phase element (CPE), and Warburg impedance (W). The larger arcs observed for CNTs/Si/C indicate higher impedance than CNTs/Si, reflecting differences in charge transfer resistance and overall electrochemical performance.

Electrochemical characteristics are essential for analyzing the behavior of working electrodes. The two primary techniques employed are CV and EIS, with their respective results displayed in Figures 9a and 9b. The corresponding equivalent circuit model is represented in Figure 9c.

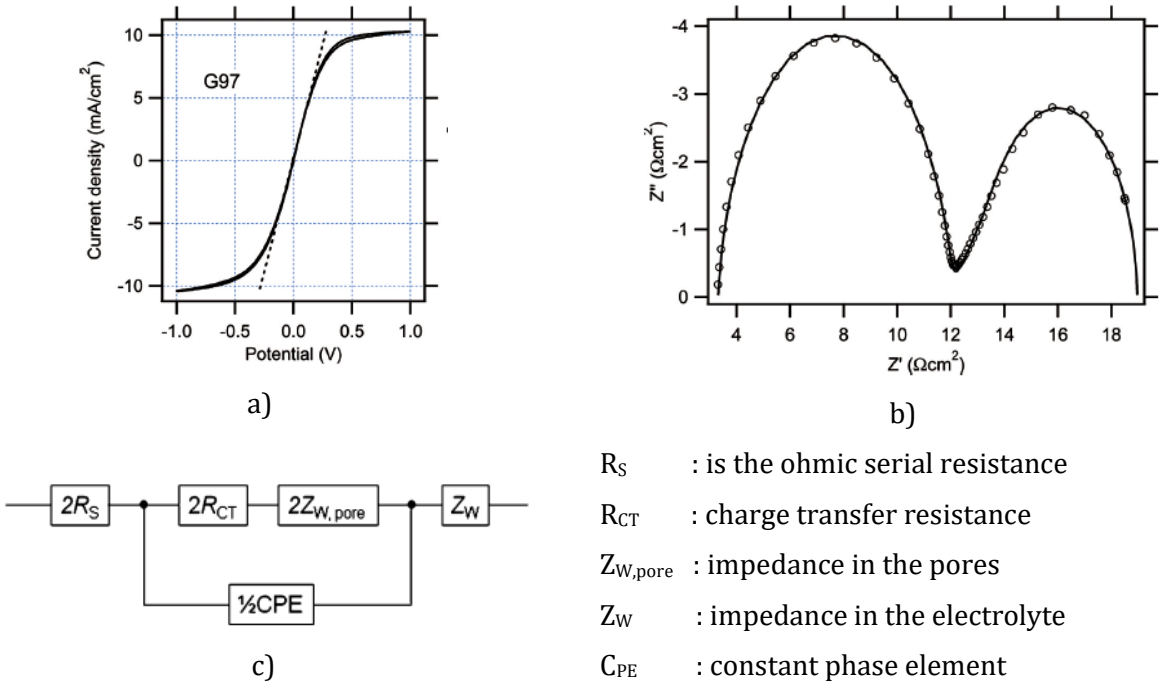

a) b)

c)

R_S : is the ohmic serial resistance

R_{CT} : charge transfer resistance

$Z_{W,pore}$: impedance in the pores

Z_W : impedance in the electrolyte

C_{PE} : constant phase element

Figure 9. (a) cyclic voltammogram, (b) electrochemical impedance measurement (EIS), (c) equivalent circuit for fitting EIS [47].

From Figure 9a, the cyclic voltammogram, several key characteristics can be derived. First, the limiting current density, governed by mass transport within the electrolyte solution, is indicated by a plateau in the cyclic voltammogram, with a value of 10.2 mA/cm^2, as shown in Figure 9a. Second, the overall cell resistance (R_{CV}) can be determined from the inverse slope at a potential of 0 V. The significance of resistance is further explored through EIS and its corresponding equivalent circuit, depicted in Figure 9b and 9c. By assigning values to each resistance and impedance element in the equivalent circuit, the solid line closely fits the experimental data from the EIS measurement. From this fitting and subsequent calculations, it becomes evident that charge transfer resistance (R_{CT}) is a critical parameter in evaluating cathode materials, as it is directly related to exchange current density. Additionally, EIS proves useful in assessing electrochemical stability, as demonstrated in Figure 10a and 10b.

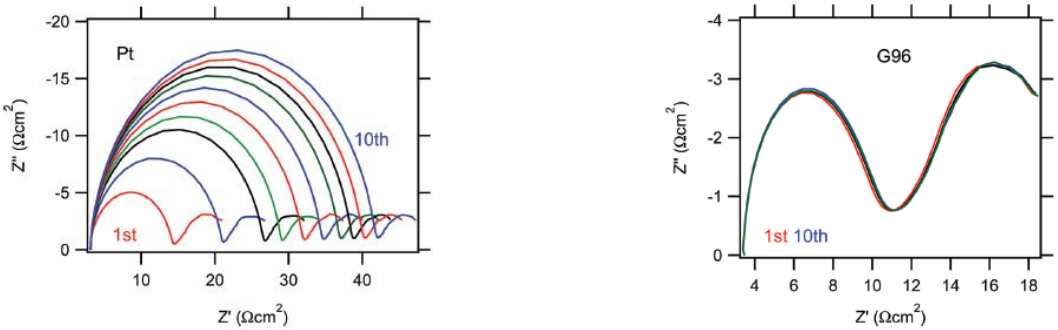

a) b)

Figure 10. (a) cycling stability of symmetrical dummy cells, (b) Nyquist Plot [47].

In Figure 10a, the Nyquist plot illustrates the electrochemical impedance spectra for a Pt electrode over multiple cycles, with particular emphasis on the 1st and 10th cycles. The semicircles reflect charge transfer resistance, and the gradual changes in arc shape over the cycles suggest variations in the electrode's electrochemical properties, possibly indicating increased resistance or degradation with cycling. The shift from the 1st to the 10th cycle points to evolving interfacial processes and potential electrode degradation over time. In contrast, Figure 10b shows the electrochemical impedance spectra for the G96 electrode across the 1st and 10th cycles. Unlike the typical semicircle, this plot displays a more complex shape, signifying the involvement of multiple electrochemical processes or interfaces. The similarity between the 1st and 10th cycles suggests stable impedance behavior, with minimal changes in charge transfer resistance or interfacial properties, indicating the G96 electrode's good durability and consistent performance across cycles.

In illustrating electrochemical impedance measurements, constructing an equivalent circuit, as shown in Figure 9c, can be quite challenging. Defining the components should take into account experimental factors such as the morphology of the electrode and the type of electrolyte used. The equivalent circuit depicted in Figure 8c mimics the morphology, incorporating impedance contributions from both the pores and the electrolyte. Researchers are increasingly examining the micro- and nano-scale structures to establish fundamental models for fabricating higher efficiency of DSSCs. An example of DSSC morphology identification is illustrated in Figure 11.

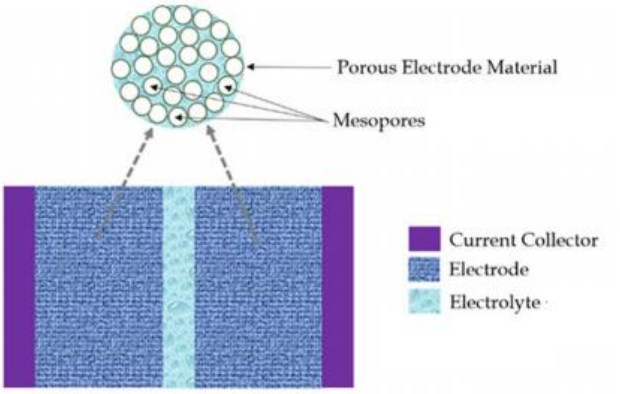

Figure 11. dummy cell likes capacitor with porous electrode [48].

Figure 11 depicts a dummy cell, akin to a capacitor, illustrating these contributions. This discussion concludes that understanding the relationship between the equivalent circuit of EIS and the cell's morphology is valuable for developing advanced devices. Enhancing the efficiency of DSSCs can be achieved by identifying optimal resistances calculated from EIS data and selecting the most effective materials. Previously, it was noted that there is a relationship between current density and mass transport as seen in cyclic voltammograms, as well as a relationship between exchange current density and charge transfer resistance in EIS. These relationships are generally explained through specific equations, with the relationship between current density and mass transport described by Equation 7.

$$j_L = \frac{2nFcD}{\delta} \tag{7}$$

In Equation 7, n represents the number of electrons, F is the Faraday constant, c is the concentration, D is the diffusion coefficient, and δ is the distance between the electrodes in a dummy cell. Selecting an electrolyte with a higher diffusion coefficient can lead to an increase

in current density. Furthermore, the relationship between current density and charge transfer resistance is outlined by Equation 8.

$$j_0 = \frac{RT}{nFR_{CT}} \quad (8)$$

In Equation 8, R represents the gas constant,T is the temperature,n denotes the number of electrons,F is the Faraday constant, and R_{CT} is the charge-transfer resistance. This equation suggests that an increase in charge-transfer resistance will result in a decrease in exchange current density. [48].

CONCLUSION

Electrochemical techniques are essential for enhancing the performance of dye-sensitized solar cells (DSSCs). Key methods include cyclic voltammetry, current-voltage (I-V) measurements, impedance spectroscopy, and Tafel polarization. I-V measurements offer valuable information on efficiency and fill factor, with optimization achieved by refining both current and voltage. Current improvements depend on factors like molecular orbitals, energy levels of materials, electrolyte diffusivity, and charge transfer resistance, while voltage is primarily influenced by molecular orbitals. Voltammetry aids in analyzing electrolyte diffusivity and assessing current density, whereas Tafel polarization highlights electrochemical catalytic activity at the electrode interface. Electrochemical Impedance Spectroscopy (EIS) plays a crucial role in evaluating charge transfer resistance, impacting stability and enabling performance optimization by connecting material properties to cell morphology. Current electrochemical techniques, while valuable for analyzing DSSCs, have limitations such as sensitivity to environmental conditions and complex data interpretation, especially in methods like EIS. Future innovations may focus on real-time, precise characterization techniques, such as in-situ spectroscopy, to enhance the accuracy and understanding of nanoscale processes. These advancements will significantly impact DSSC research and development, enabling the design of more efficient and stable materials with lower charge transfer resistance, leading to the creation of longer-lasting, more cost-effective solar cells.

REFERENCES

[1] "IEA PVPS report - Trends in Photovoltaic Applications 2019," 2019, doi: 10.13140/RG.2.2.10332.00647.

[2] N. Kutlu, "Investigation of electrical values of low-efficiency dye-sensitized solar cells (DSSCs)," *Energy*, vol. 199, p. 117222, 2020, doi: https://doi.org/10.1016/j.energy.2020.117222.

[3] K. Sharma, V. Sharma, and S. S. Sharma, "Dye-Sensitized Solar Cells: Fundamentals and Current Status," 2018, *Springer New York LLC*. doi: 10.1186/s11671-018-2760-6.

[4] S. Assegaf, "Highest Efficiency Dssc Fabrication With Natural Dye and Chemical Dye," *International Journal of Education, Information Technology, and Others*, vol. 7, no. 2, pp. 266–238, 2024, doi: 10.5281/zenodo.11195100.

[5] A. Rais and Y. Warti, "Analysis of DSSC (dye sensitized solar cell) and characterization of ZnO-TiO2 semiconductor using method sol-gel as a material solar cell," *J Phys Conf Ser*, vol. 2193, no. 1, p. 012093, 2022, doi: 10.1088/1742-6596/2193/1/012093.

[6] A. J. Riquelme *et al.*, "Characterization of Photochromic Dye Solar Cells Using Small-Signal Perturbation Techniques," *ACS Appl Energy Mater*, vol. 4, no. 9, pp. 8941–8952, Sep. 2021, doi: 10.1021/acsaem.1c01204.

[7] J. Gao, A. Tot, H. Tian, J. M. Gardner, D. Phuyal, and L. Kloo, "Electrochemical impedance and X-ray absorption spectroscopy analyses of degradation in dye-sensitized solar cells containing cobalt tris(bipyridine) redox shuttles," *Physical Chemistry Chemical Physics*, vol. 24, no. 31, pp. 18888–18895, Jul. 2022, doi: 10.1039/d2cp02283d.

[8] A. C. Lazanas and M. I. Prodromidis, "Electrochemical Impedance Spectroscopy—A Tutorial," Jun. 21, 2023, *American Chemical Society*. doi: 10.1021/acsmeasuresciau.2c00070.

[9] Md. K. Nazeeruddin, E. Baranoff, and M. Grätzel, "Dye-sensitized solar cells: A brief overview," *Solar Energy*, vol. 85, no. 6, pp. 1172–1178, 2011, doi: https://doi.org/10.1016/j.solener.2011.01.018.

[10] Masud and H. K. Kim, "Redox Shuttle-Based Electrolytes for Dye-Sensitized Solar Cells: Comprehensive Guidance, Recent Progress, and Future Perspective," *ACS Omega*, vol. 8, no. 7, pp. 6139–6163, Feb. 2023, doi: 10.1021/acsomega.2c06843.

[11] Z. Agheli, M. Pordel, and S. A. Beyramabadi, "Synthesis, characterization, optical properties, computational characterizations, QTAIM analysis and cyclic voltammetry of new organic dyes for dye-sensitized solar cells," *J Mol Struct*, vol. 1202, Feb. 2020, doi: 10.1016/j.molstruc.2019.127228.

[12] P. Setiarso, R. V. Harsono, and N. Kusumawati, "Fabrication of Dye Sensitized Solar Cell (DSSC) Using Combination of Dyes Extracted from Curcuma (Curcuma xanthorrhiza) Rhizome and Binahong (Anredera cordifolia) Leaf with Treatment in pH of the Extraction," *Indonesian Journal of Chemistry*, vol. 23, no. 4, pp. 924–936, 2023, doi: 10.22146/ijc.77860.

[13] F. Arjmand, Z. Rashidi Ranjbar, and H. Fatemi E. G, "Effect of dye complex structure on performance in DSSCs; An experimental and theoretical study," *Heliyon*, vol. 8, no. 11, Nov. 2022, doi: 10.1016/j.heliyon.2022.e11692.

[14] H. A. Deepa, G. M. Madhu, and B. E. K. Swamy, "Evaluation of performance characteristics of nano TiO2and TiO2-ZnO composite for DSSC applications and electrochemical determination of potassium ferrocyanide using cyclic voltammetry," *Mater Res Express*, vol. 8, no. 12, Dec. 2021, doi: 10.1088/2053-1591/ac3e27.

[15] C. Fengxiang, A. Yu, W. Jiafu, and W. Lisheng, "The I-V Measurement System for Solar Cells Based on MCU," *J Phys Conf Ser*, vol. 276, no. 1, p. 012161, 2011, doi: 10.1088/1742-6596/276/1/012161.

[16] A. M. Abdel-Maksood and F. A. S. Soliman, "Performance Dependence of (I-V) and (C-V) for Solar Cells on Environmental Conditions," 2018. [Online]. Available: https://api.semanticscholar.org/CorpusID:212532196

[17] S. Visnupriya, N. Prabavathi, and P. Vijayakumar, "Ni-Mo bimetallic oxides/rGO nanocomposites as counter electrode for the application of DSSCs," *Chemical Physics Impact*, vol. 8, p. 100598, 2024, doi: https://doi.org/10.1016/j.chphi.2024.100598.

[18] D. Kumar Sharma and G. Purohit, "Fill Factor based Maximum Power Point Tracking (MPPT) for Standalone Solar PV System Sustainable Innovations Welfare Society (SIWS) Meerut INDIA Fill Factor Based Maximum Power Point Tracking (MPPT) for Standalone Solar PV System," 2013. [Online]. Available: https://www.researchgate.net/publication/259757513

[19] S. Khunchan and B. Wiengmoon, "Method to determine the single curve IV characteristic parameter of solar cell," *J Phys Conf Ser*, vol. 1144, no. 1, p. 012012, 2018, doi: 10.1088/1742-6596/1144/1/012012.

[20] F. Dincer and M. E. Meral, "Critical Factors that Affecting Efficiency of Solar Cells," *Smart Grid and Renewable Energy*, vol. 1, pp. 47–50, 2010, [Online]. Available: https://api.semanticscholar.org/CorpusID:27708847

[21] M. H. Wolfe, "Efficiency in Solar Cells," 2013. [Online]. Available: https://api.semanticscholar.org/CorpusID:18357653
[22] W. Shockley and H. J. Queisser, "Detailed Balance Limit of Efficiency of p-n Junction Solar Cells," *J Appl Phys*, vol. 32, no. 3, pp. 510–519, Mar. 1961, doi: 10.1063/1.1736034.
[23] J. M. Greulich, M. Glatthaar, and S. Rein, "Fill factor analysis of solar cells' current–voltage curves," *Progress in Photovoltaics: Research and Applications*, vol. 18, 2010, [Online]. Available: https://api.semanticscholar.org/CorpusID:98270169
[24] A. Yildiz *et al.*, "Efficient Iron Phosphide Catalyst as a Counter Electrode in Dye-Sensitized Solar Cells," *ACS Appl Energy Mater*, vol. 4, no. 10, pp. 10618–10626, Oct. 2021, doi: 10.1021/acsaem.1c01628.
[25] Y. Zhang, P. Wang, T. Zhang, and B. Gou, "High-Efficiency Dye-Sensitized Solar Cells Based on Kesterite Cu2ZnSnSe4Inlaid on a Flexible Carbon Fabric Composite Counter Electrode," *ACS Omega*, vol. 5, no. 38, pp. 24898–24905, Sep. 2020, doi: 10.1021/acsomega.0c03686.
[26] D. Nan, H. Fan, A. Bolag, W. Liu, and T. Bao, "Enhanced electrocatalytic properties in dye-sensitized solar cell via Pt/SBA-15 composite with optimized Pt constituent," *Heliyon*, vol. 9, no. 11, p. e22403, 2023, doi: https://doi.org/10.1016/j.heliyon.2023.e22403.
[27] *ICECDS : 2017 International Conference on Energy, Communication, Data Analytics and Soft Computing : 1-2 August 2017, Chennai, India*. Institute of Electrical and Electronics Engineers, 2018.
[28] N. Kanjana *et al.*, "Fly ash boosted electrocatalytic properties of PEDOT:PSS counter electrodes for the triiodide reduction in dye-sensitized solar cells," *Sci Rep*, vol. 13, no. 1, Dec. 2023, doi: 10.1038/s41598-023-33020-6.
[29] J. Mohammadian, S. Osfouri, T. Jalali, and A. Jamekhorshid, "Electrochemical impedance spectroscopy analysis of dye-sensitized solar cells composed of electrospun composite photoanodes: A comparative study of natural and synthetic sensitizers," *Optik (Stuttg)*, vol. 303, p. 171730, 2024, doi: https://doi.org/10.1016/j.ijleo.2024.171730.
[30] A. Ch. Lazanas and M. I. Prodromidis, "Electrochemical Impedance Spectroscopy—A Tutorial," *ACS Measurement Science Au*, vol. 3, no. 3, pp. 162–193, Jun. 2023, doi: 10.1021/acsmeasuresciau.2c00070.
[31] A. J. Riquelme *et al.*, "Characterization of Photochromic Dye Solar Cells Using Small-Signal Perturbation Techniques," *ACS Appl Energy Mater*, vol. 4, no. 9, pp. 8941–8952, Sep. 2021, doi: 10.1021/acsaem.1c01204.
[32] W. Rahmalia, I. H. Silalahi, T. Usman, J. F. Fabre, Z. Mouloungui, and G. Zissis, "Stability, reusability, and equivalent circuit of TiO2/treated metakaolinite-based dye-sensitized solar cell: effect of illumination intensity on V oc and I sc values," *Mater Renew Sustain Energy*, vol. 10, no. 2, Jun. 2021, doi: 10.1007/s40243-021-00195-9.
[33] S. Sahu, M. Patel, A. K. Verma, and S. Tiwari, "Analytical study of current density-voltage relation in dye-sensitized solar cells using equivalent circuit model," in *2017 International Conference on Energy, Communication, Data Analytics and Soft Computing (ICECDS)*, 2017, pp. 1489–1493. doi: 10.1109/ICECDS.2017.8389693.
[34] J. Gao, A. Tot, H. Tian, J. M. Gardner, D. Phuyal, and L. Kloo, "Electrochemical impedance and X-ray absorption spectroscopy analyses of degradation in dye-sensitized solar cells containing cobalt tris(bipyridine) redox shuttles," *Physical Chemistry Chemical Physics*, vol. 24, no. 31, pp. 18888–18895, Jul. 2022, doi: 10.1039/d2cp02283d.
[35] M. A. Varnosfaderani and D. Strickland, "Online Electrochemical Impedance Spectroscopy (EIS) estimation of a solar panel," *Vacuum*, vol. 139, pp. 185–195, 2017, doi: https://doi.org/10.1016/j.vacuum.2017.01.011.

[36] S. Sarker, A. J. S. Ahammad, H. W. Seo, and D. M. Kim, "Electrochemical Impedance Spectra of Dye-Sensitized Solar Cells: Fundamentals and Spreadsheet Calculation," *International Journal of Photoenergy*, vol. 2014, pp. 1–17, 2014, [Online]. Available: https://api.semanticscholar.org/CorpusID:55158383

[37] J. Gao, A. Tot, H. Tian, J. M. Gardner, D. Phuyal, and L. Kloo, "Electrochemical impedance and X-ray absorption spectroscopy analyses of degradation in dye-sensitized solar cells containing cobalt tris(bipyridine) redox shuttles," *Physical Chemistry Chemical Physics*, vol. 24, no. 31, pp. 18888–18895, Jul. 2022, doi: 10.1039/d2cp02283d.

[38] M. S. H. Choudhury, S. E. Ahmed Himu, M. U. Khan, M. Z. Hasan, M. S. Alam, and T. Soga, "Analysis of charge transport resistance of ZnO-based DSSCs because of the effect of different compression temperatures," *AIP Adv*, vol. 13, no. 9, p. 095129, Sep. 2023, doi: 10.1063/5.0166767.

[39] V. A. González-Verjan *et al.*, "Effect of TiO2 particle and pore size on DSSC efficiency," *Mater Renew Sustain Energy*, vol. 9, no. 2, Jul. 2020, doi: 10.1007/s40243-020-00173-7.

[40] R. Agarwal, Y. Vyas, P. Chundawat, Dharmendra, and C. Ameta, "Outdoor Performance and Stability Assessment of Dye-Sensitized Solar Cells (DSSCs)," in *Solar Radiation*, M. Aghaei, Ed., Rijeka: IntechOpen, 2021, p. Ch. 7. doi: 10.5772/intechopen.98621.

[41] M. Becker, M. S. Bertrams, E. C. Constable, and C. E. Housecroft, "How reproducible are electrochemical impedance spectroscopic data for dye-sensitized solar cells?," *Materials*, vol. 13, no. 7, Apr. 2020, doi: 10.3390/ma13071547.

[42] S. Rudra, H. W. Seo, S. Sarker, and D. M. Kim, "Simulation and electrochemical impedance spectroscopy of dye-sensitized solar cells," *Journal of Industrial and Engineering Chemistry*, vol. 97, pp. 574–583, 2021, doi: https://doi.org/10.1016/j.jiec.2021.03.010.

[43] A. E. Touihri, T. Azizi, and R. Gharbi, "Autonomous I-V and Electrochemical Impedance Spectroscopy characterization system for Dye Sensitized Solar Cells," in *Proceedings of the International Conference on Advanced Systems and Emergent Technologies, IC_ASET 2020*, Institute of Electrical and Electronics Engineers Inc., Dec. 2020, pp. 235–240. doi: 10.1109/IC_ASET49463.2020.9318312.

[44] M. Z. H. Khan, M. R. Al-Mamun, P. K. Halder, and M. A. Aziz, "Performance improvement of modified dye-sensitized solar cells," *Renewable and Sustainable Energy Reviews*, vol. 71, pp. 602–617, 2017, doi: https://doi.org/10.1016/j.rser.2016.12.087.

[45] K. Kakiage, Y. Aoyama, T. Yano, K. Oya, J. Fujisawa, and M. Hanaya, "Highly-efficient dye-sensitized solar cells with collaborative sensitization by silyl-anchor and carboxy-anchor dyes," *Chemical Communications*, vol. 51, no. 88, pp. 15894–15897, 2015, doi: 10.1039/C5CC06759F.

[46] Z. Yang, Y. Xia, J. Ji, B. Qiu, K. Zhang, and Z. Liu, "Superior cycling performance of a sandwich structure Si/C anode for lithium ion batteries," *RSC Adv*, vol. 6, no. 15, pp. 12107–12113, 2016, doi: 10.1039/C5RA23283J.

[47] L. Kavan, J.-H. Yum, and M. Grätzel, "Graphene Nanoplatelets Outperforming Platinum as the Electrocatalyst in Co-Bipyridine-Mediated Dye-Sensitized Solar Cells," *Nano Lett*, vol. 11, no. 12, pp. 5501–5506, Dec. 2011, doi: 10.1021/nl203329c.

[48] L. Kavan, J.-H. Yum, and M. Graetzel, "Graphene-based cathodes for liquid-junction dye sensitized solar cells: Electrocatalytic and mass transport effects," *Electrochim Acta*, vol. 128, pp. 349–359, 2014, doi: https://doi.org/10.1016/j.electacta.2013.08.112.